The Astrophysical Journal Letters, 843:L25 (6pp), 2017 July 10 https://doi.org/10.3847/2041-8213/aa7aec

Prediction for the Flow-induced Gravity Field of Saturn: Implications for *Cassini*'s Grand Finale

Eli Galanti and Yohai Kaspi
Department of Earth and Planetary Sciences, Weizmann Institute of Science, Rehovot, Israel; eli.galanti@weizmann.ac.il
Received 2017 April 23; revised 2017 June 4; accepted 2017 June 19; published 2017 July 7

Abstract

The *Cassini* measurements of Saturn's gravity field during its Grand Finale might shed light on a long-standing question regarding the flow on Saturn. While the cloud-level winds are well known, little is known about whether these winds are confined to the outer layers of the planet or penetrate deep into the interior. An additional complexity is added by the uncertainty in the exact rotation period of Saturn, a key factor in determining the cloud-level winds, with an effect on the north–south symmetric part of the winds. Using Saturn's cloud-level winds we relate the flow to the gravity harmonics. We give a prediction for the odd harmonics J_3, J_5, J_7, and J_9 as a function of the flow depth, identifying three ranges of depths. Since the odd harmonics depend solely on the flow, and are not influenced by Saturn's shape and static density distribution, any measured value of the odd harmonics by *Cassini* can be used to uniquely determine the depth of the flow. We also discuss the flow-induced even harmonics ΔJ_2, ΔJ_4,…,ΔJ_{12} that are affected by Saturn's rotation period. While the high-degree even harmonics might also be used to determine the flow depth, the lower-degree even harmonics serve as uncertainties for analysis of the planet's interior structure and composition. Thus, the gravity harmonics measured during the *Cassini* Grand Finale may be used to get a first-order estimate of the flow structure and to better constrain the planet's density structure and composition.

Key words: gravitation – hydrodynamics – planets and satellites: atmospheres – planets and satellites: gaseous planets – planets and satellites: individual (Saturn)

1. Introduction

Broad and strong winds exist at the cloud level of Saturn, with zonal flows that reach nearly 500 m s^{-1} (e.g., Sanchez-Lavega et al. 2000; Garcia-Melendo et al. 2011). These measurements are well established, but how deep the winds penetrate into the planet interior remains unknown. They might extend inward tens of kilometers, a mere fraction of the planet's radius of more than 60,000 km, or thousands of kilometers deep into the planet's interior, swirling a considerable part of its mass. The Grand Finale phase of the NASA spacecraft *Cassini* might shed new light on this question. Between 2017 May and August, *Cassini* will perform multiple close flybys of Saturn and its proximity to the planet's cloud level will allow for high-precision measurements of its gravity field, with emphasis on the gravity field's latitudinal variations.

The connection between the flow within a gas giant and its gravity field was studied extensively during the past two decades. Due to the rapid rotation of the planet, the large-scale flow is likely, to leading order, in geostrophic balance (e.g., Pedlosky 1987), resulting in thermal wind balance between the flow and an anomalous density field. This balance allows for using the gravity field measurements on either Jupiter or Saturn to infer the flow structure below the planet's cloud level (Hubbard 1999; Kaspi et al. 2010). The relation between a depth-dependent flow field on Saturn and its gravity field was first discussed by Kaspi (2013), who developed a method to estimate the zonal gravity harmonics under baroclinic conditions. In that study, a solution for the odd gravity harmonics was given as function of the depth of the flow, allowing for the estimation of the depth of the winds given the expected gravity measurements from *Cassini*. However, during the past few years (mostly in connection to the Juno mission) this methodology was further developed to allow more accurate solutions (Galanti & Kaspi 2016; Kong et al. 2016; Galanti et al. 2017b); hence, a revision and elaboration of these results is in place.

Furthermore, another critical aspect of the problem was not discussed in Kaspi (2013). The rotation period of Saturn, a key parameter in determining the cloud-level winds (Sanchez-Lavega et al. 2000), is still not known with high certainty (Helled et al. 2015). While *Voyager* measured a rotation period of 10 hr 39 minutes 22 s (Smith et al. 1982), the *Cassini* measurements yield a higher value of 10 hr 45 minutes 45 s ± 36 s (Gurnett et al. 2005). Recent studies suggested that the rotation period might be much shorter, with estimates of 10 hr 32 minutes 35 s ± 13 s (Anderson & Schubert 2007), 10 hr 34 minutes 13 s ± 20 s (Read et al. 2009), and 10 hr 32 minutes 45 s ± 46 s (Helled et al. 2015). All of these studies either relied entirely on cloud-level winds, assumed a specific range of internal density structure, or relied on exact knowledge of the planet's shape. Considering the uncertainties associated with current knowledge on the interior density structure of Saturn and its planetary shape, Helled et al. (2015) concluded that a rotation period of 10 hr 34 minutes 22 s ± 3.5 minutes might be most appropriate until further measurements are obtained. The different estimates are summarized in Table 1.

In this study, we present a prediction of the wind-related gravity field of Saturn, given a range of possible penetration depths and taking into account the uncertainty in Saturn's rotation period. We discuss the two groups of harmonics—the odd gravity harmonics, whose key advantage is in their sole dependence on the north–south asymmetry in the flow field. They are not affected by the internal static density structure or planetary shape and are not affected by the uncertainty in the rotation period. The second group is composed from the even harmonics. The high even harmonics $n > 8$ (Kaspi 2013) might have a measurable contribution from the flow since the

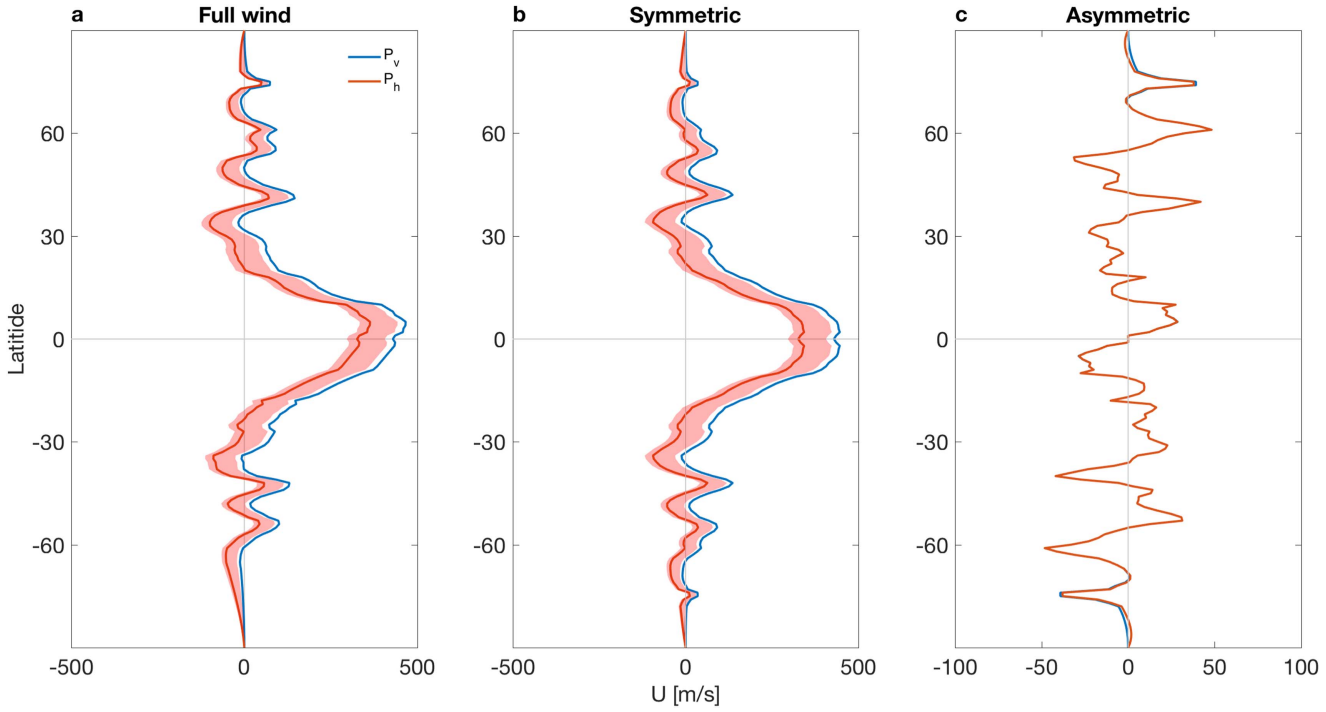

Figure 1. (a) Saturn cloud-level wind calculated with respect to P_v (blue line) and P_h (red line). Also shown is a light red shading is the wind range based on P_h^+ and P_h^-. (b) Same as (a), but for the north–south symmetric part of the wind. (c) North–south asymmetric part of the wind.

Table 1
The Different Estimations of Saturn's Rotation Period Used in This Study

Source	Observations/Theory Used	Rotation Period	Symbol
Smith et al. (1982)	Kilometric radiation	10 hr 39 minutes 22 s ± 7 s	P_v
Helled et al. (2015)	Gravity, shape, and internal structure	10 hr 32 minutes 45 s ± 46 s	$P_{\rm h}$
	Gravity and shape	10 hr 34 minutes 22 s ± 3 minutes	$P_{\rm h}^a$ ($P_{\rm h}^+$, $P_{\rm h}^-$)
Gurnett et al. (2005)	Kilometric radiation	10 hr 45 minutes 45 s ± 36 s	Not used here
Anderson & Schubert (2007)	Gravity, shape, and wind	10 hr 32 minutes 35 s ± 13 s	Not used here
Read et al. (2009)	Wind (potential vorticity)	10 hr 34 minutes 13 s ± 20 s	Not used here

Note. $P_{\rm h}^+$ and $P_{\rm h}^-$ refer to the upper and lower uncertainty limits, respectively, of $P_{\rm h}^a$.

static contribution decays rapidly for the high-degree harmonics, while the lower-degree harmonics contribution from the flow can be used to better constrain models of Saturn's interior structure and composition (e.g., Fortney & Nettelmann 2010; Guillot 2005; Wahl et al. 2017).

The Letter is organized as follows: in Section 2, we present the cloud-level wind data and the dynamical balance used to establish the connection to the gravity field. In Section 3, we discuss the solutions for the asymmetric and symmetric parts of the gravity field, presenting a prediction to what might be the results from *Cassini* and how they can be interpreted. We conclude in Section 4.

2. Data and Models

2.1. Saturn Surface Wind and the Uncertainty in the Planet's Rotation Period

Similar to Jupiter, on Saturn we have good measurements of the cloud-level winds. The observed zonal winds on Saturn as reported by Sanchez-Lavega et al. (2000) are shown in Figure 1 (blue lines). They consist of a strong, wide, and mostly hemispherically symmetric eastward jet around the equator (Figure 1(b)) and a series of jets that have north–south symmetric, as well as antisymmetric, components in both hemispheres (Figures 1(b), (c)).

These winds were reported with respect to the *Voyager* measured rotation period. Since the Saturn rotation period is still unknown to sufficient accuracy, we need to examine how the wind is affected by the specific choice of the rotation period. The Sanchez-Lavega et al. (2000) winds can be calibrated with respect to any rotation period using

$$U_0(\theta) = U_v(\theta) + 2\pi(P_v^{-1} - P_0^{-1})R_g(\theta)\sin(\theta), \quad (1)$$

where P_0 is the new reference rotation period, θ is the planetocentric latitude, and R_g is the geoid shape of the planet, calculated following Sanchez-Lavega et al. (2000, their Equation (2)).

The re-calibrated wind based on P_h is shown in Figure 1 (red lines), and the winds based on the range of rotation periods between P_h^+ and P_h^- are shown as the red shaded areas. Since

the geoid R_g is symmetric, shifting the winds from one rotation period to another affects only the symmetric part of the wind (Figure 1(b)) and has no effect on the asymmetric part (Figure 1(c)).

2.2. Relating the Cloud-level Wind to the Gravity Field

The underlying assumption taken is that, to leading order, conservation of angular momentum inhibits, to leading order, the mixing of momentum across lines parallel to the axis of rotation (Kaspi et al. 2009; Schneider & Liu 2009; Liu et al. 2014); therefore, the observed cloud-level zonal winds are projected inward along these lines. What is unknown and to be determined by the *Cassini* measurements is the depth to which the flow penetrates. For simplicity we assume that the flow decays exponentially toward the planet center in the radial direction

$$U(r,\theta) = U_0(\theta)\exp\left[-\frac{R-r}{H}\right], \quad (2)$$

where H is the decay scale setting the depth of the flow, $R = 58{,}232$ km is the mean Saturn radius, and r is the radial distance from the planet center. The exponential function is an arbitrary choice and when the *Cassini* measurements arrive other decay functions should be examined to reach the best fit between the model gravity harmonics and those measured. Note, however, that the results presented here are not altered significantly by the usage of other decay functions.

Assuming that the large-scale dynamics obey a geostrophic balance between the pressure gradient force and the Coriolis force (Pedlosky 1987; Kaspi et al. 2009), and that to leading order the flow is longitudinally symmetric, the governing equation for the balance between the flow field and the density perturbation is

$$\frac{4\pi}{P_0}\frac{\partial}{\partial z}(\tilde{\rho}U) = g_0\frac{\partial}{\partial\theta}\rho', \quad (3)$$

where P_0 is the planetary rotation period, $\tilde{\rho}(r)$ is the background density field, $g_0(r)$ is the mean gravity acceleration in the radial direction, $\rho'(r,\theta)$ is the density anomaly associated with the flow field, and z is the direction parallel to the axis of rotation. Given a cloud-level wind and a decay depth H, Equation (3), together with Equation (2), is solved for the density in a method similar to that used in Galanti et al. (2017a). Note that changing the planetary rotation period from one reference value to another has a negligible effect ($\sim$1%) on the balance of Equation (3). Also note that while the oblateness of Saturn might affect some gravity harmonics (Zhang et al. 2015; Cao & Stevenson 2017), for the leading-order calculation of the harmonics sphericity can be assumed to good accuracy (Galanti et al. 2017b). The gravity harmonics are then integrated from the density field

$$\Delta J_n = -\frac{2\pi}{MR^n}\int_0^R r^{n+2}dr\int_{\mu=-1}^{1}P_n(\mu)\rho'(r,\mu)d\mu, \quad (4)$$

where ΔJ_n, $n = 2,\ldots,N$ are the coefficients of the gravity harmonics, M is the planetary mass, P_n are the Legendre polynomials, and $\mu = \cos(\theta)$. The solution for Equation (3) gives the density perturbations up to an integration function ${\rho'}_0(r)$ that depends on r but not on θ. This unknown part of the density field has no effect on the zonal harmonics since

$$\Delta J_n = -\frac{2\pi}{MR^n}\int_0^R r^{n+2}{\rho_0}'(r)dr\int_{\mu=-1}^{1}P_n(\mu)d\mu = 0, \quad (5)$$

which vanishes due to the Legendre polynomials having a zero latitudinal mean for any value of n (Kaspi et al. 2016).

In order to assist the analysis of the gravity harmonics (Sections 3.1 and 3.2), solutions for the density field are shown in Figure 2, for two reference rotation periods (P_v and P_h) and three representative depths (100 km, 500 km, and 1000 km). Since our goal is to understand the relation between a given flow field and the gravity harmonics, the density field shown is normalized by the sine of the latitude, and by $(r/R_m)^3$ so that the density at the surface of the planet at the equator is not changed by the normalization. The normalization is chosen to reflect the dependence of the gravity harmonics on the density (Equation (4)), so that aside from multiplication by a constant, a simple summation is all that is needed to go from the normalized density shown in Figure 2 to the gravity harmonics.

3. Results

3.1. The Asymmetric Gravity Field

The Saturn asymmetric gravity field is attributed in full to the flow field (Kaspi 2013). While most of the amplitude of the even gravity harmonics originates from the deviation of the planetary shape from sphericity and its internal density distribution (at least up to J_8), there is no contribution from the static body of Saturn to the odd gravity harmonics. Therefore, any odd zonal harmonics measured by *Cassini* will give a direct indication to the structure and depth of the flow so that our prime goal is to give a prediction for the odd gravity harmonics. As expected from the analysis of the cloud-level wind (Figures 1(b), (c)), knowledge of the exact planetary rotation period is not a prerequisite for the calculation of the odd gravity harmonics. This is another advantage of using the odd harmonics to estimate the flow structure.

Solving Equation (3) for different decay depths reveals the range of odd zonal harmonics J_3, J_5, J_7, and J_9 that might be expected to be measured in Saturn (Figure 3). Remarkably, all four harmonics show similar behavior with three depth ranges defining the expected values. Given a shallow flow, with decay depth ranging from zero to around 300 km, the odd harmonics have negative values of up to -10^{-8}. Flow structures with decay depths larger than 900 km result in all odd harmonics being positive with values of up to 10^{-6} for J_3 and J_5. In between decay depths of 300 to 900 km (Figure 3, shaded area) the odd gravity harmonics change their sign. Note that unanimous change of sign for all four harmonics is specific to Saturn and is not the case for Jupiter (Kaspi 2013).

The sign change of the harmonics when the depth of the flow increases is a result of the changing density structure (Figure 2). When the flow is shallow ($H = 100$ km), the density perturbations (Figures 2(a), (b)) are in opposite sign to the integrated flow structure (due to the nature of Equation (3); see Section 2.2). Then, for intermediate depths ($H = 500$ km) there exist two regions of density perturbations with opposite signs (Figures 2(c), (d)) that result in the gravity harmonics flipping sign. Finally, for flows penetrating deep into the planet's interior ($H = 100$ km) the expected sign of the density perturbations dominates (Figures 2(e), (f)) and so the gravity harmonics get their high positive values. Note again that even

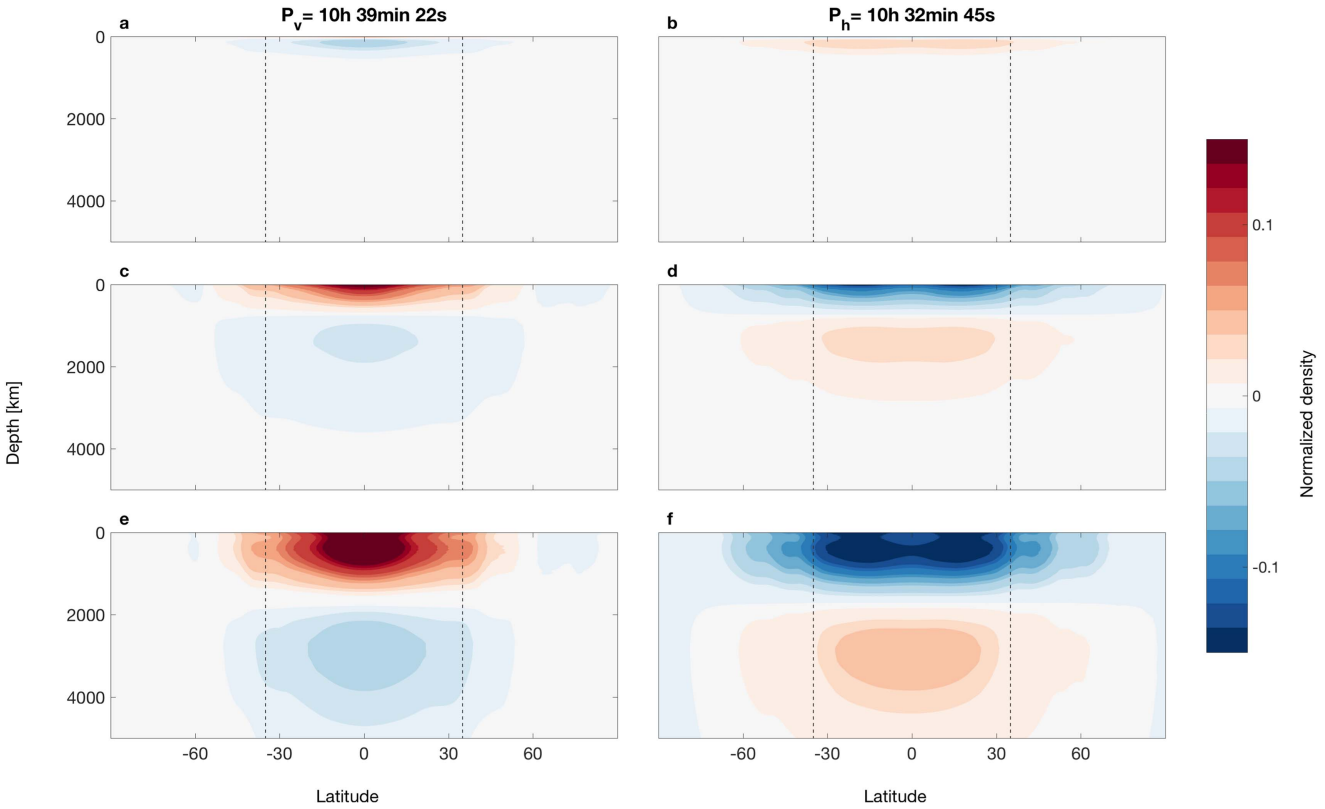

Figure 2. Anomalous density field normalized to show the direct effect on the gravity harmonics. Shown are three cases for decay depths $H = 100$ km ((a), (b)), $H = 500$ km ((c), (d)), and $H = 1000$ km ((e), (f)). Left panels are for surface winds based on $P_v = 10$ h 39 minutes 22 s, and right panels are for $P_h = 10$ h 32 minutes 45 s. The dashed lines indicate the zero crossing of the J_2 gravity harmonic.

though the density structures have profoundly different structures based on different reference rotation periods (Figures 2(a), (c), (e) versus Figures 2(b), (d), (f)), the odd gravity harmonics are not affected by these differences.

3.2. The Symmetric Gravity Field

The even gravity harmonics should be divided into two parts. The low harmonics, up to J_8, are dominated by the static body of Saturn (e.g., Kaspi et al. 2016), so that the flow-induced signal is not expected to be deciphered by the *Cassini* measurements. However, estimating the range of the flow-induced even harmonics can be used as uncertainties to better constrain the models of Saturn's internal density structure and composition (e.g., Guillot 2005; Wahl et al. 2017). The flow-induced signal in the higher even harmonics becomes comparable in magnitude to the static component, depending on the depth of the flow, and might be deciphered from the measurements (Kaspi 2013).

Unlike the asymmetric part of the wind, the symmetric part is affected substantially by the planet's rotation period (Figure 1(b)). Therefore, in order to map the possible flow-induced even zonal harmonics, Equations (3) and (4) need to be solved not only for different decay depths, but also for different cloud-level wind profiles.

Figure 4(a) shows the even gravity harmonics as a function of the depth H, with cloud-level wind based on P_v. As with the odd harmonics, a transition depth exists between $H = 200$ km and $H = 500$ km (gray area), in which the harmonics change their sign. Also plotted are shading areas for ΔJ_4, ΔJ_6,…,ΔJ_{12} to denote the solutions with cloud-level wind based on rotation periods P_h^- and P_h^+. Aside from a region of high H values where the shading for J_4 is apparent, the shadings overall are almost indistinguishable from the solution with P_v. This is not the case for J_2, whose values given varying wind profiles are so large that they cannot be shown in Figure 4(a) and need to analyzed separately.

The overall analysis of ΔJ_2 is shown in Figure 4(b). Alongside the P_v related harmonic (black line), solutions based on the other rotation periods are shown (red lines). It is clear that for ΔJ_2 the effect of the planet's rotation period is profound—solving with P_h results in a behavior that is opposite in nature to the solution based on P_v. The source for the almost singular effect of the rotation period on ΔJ_2 is the particular shape of the planet.

The geoid R_g projection onto the Legendre polynomials ΔJ_2, ΔJ_4, and, ΔJ_6 is such that the ratio between the projections is $1 : 34 : 941$, respectively. This ratio is similar to the Saturn even zonal harmonics $J_2 = 16{,}290.17 \pm 0.27$, $J_4 = -935.83 \pm 2.77$, $J_6 = 86.14 \pm 9.64$ as reported by Jacobson et al. (2006). This means that a re-calculation of the cloud-level wind with respect to a modified rotation period creates an anomalous signal with a projection mostly on J_2; hence, the effect can be seen dramatically in the flow-induced gravity harmonic ΔJ_2 with only some minor effect on ΔJ_4 and a minuscule effect on ΔJ_6, ΔJ_8, ΔJ_{10}, and ΔJ_{12}.

4. Conclusions

In anticipation of the *Cassini* Grand Finale, we analyze the flow-related gravity field that is part of the total gravity harmonics to be measured by the spacecraft. The contributions

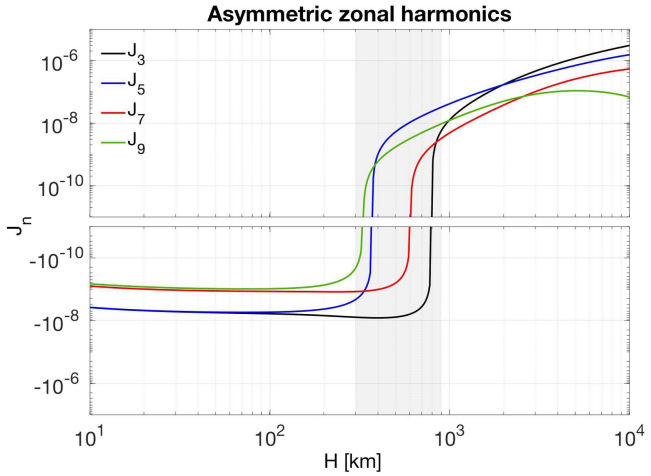

Figure 3. Solutions for the odd zonal gravity harmonics J_3, J_5, J_7, and J_9 as function of the e-folding depth of the flow. The shaded area, between $H = 300$ km and $H = 900$ km, indicates the range of flow depths in which all four harmonics change their sign from negative to positive.

to the gravity harmonics can be separated into two parts—a contribution to the low-degree even harmonics (at least up to J_8) resulting from the planet's shape deviation from a sphere (e.g., Hubbard 1982; Kaspi et al. 2016), and a contribution to both even and odd harmonics resulting from the differential flow on the planet (Kaspi 2013). The implication for the *Cassini* Grand Finale is that while the low-degree even harmonics will be dominated by the static body shape, therefore rendering them impractical for the calculation of the depth of the flow, any signal to be measured in the odd harmonics can be directly related to the flow structure.

Unlike Jupiter, the rotation period of Saturn is still not known exactly. This poses a difficulty for analyzing the flow-related gravity field as the measurements of the cloud-level winds depend on the rotation period (Sanchez-Lavega et al. 2000). Simple decomposition of the winds into their symmetric and asymmetric parts shows that the value of the rotation period affects only the symmetric part. Therefore, the asymmetric part of the flow-related gravity field will not be affected by the rotation period.

Using the measured cloud-level winds on Saturn and thermal wind balance, the flow structure is related to the zonal gravity harmonics to be measured by *Cassini*. We assume that the cloud-level wind has a penetration depth so that a mapping can be done between the depth of the flow and the resulting gravity harmonics. We calculate the odd and even zonal gravity harmonics and analyze the results with respect to the rotation-period-dependent flow structure.

We give a prediction for the odd gravity harmonics J_3, J_5, J_7, and J_9 as function of the depth of the flow. Three ranges of decay depths are identified—shallow flows with depths of up to $H = 300$ km where all four odd harmonics are negative, deep flows with $H > 900$ km where all four harmonics are positive, and a range between $H = 300$ km and $H = 900$ km where the harmonics change sign. This behavior is found to be a result of the specific structures of the density field that is in balance with the flows. Note that each measured odd harmonic independently can give the depth of the flow based on this model, and the combination of them should confirm the results. With more gravity harmonics obtained by *Cassini*, more sophisticated flow structures could be matched.

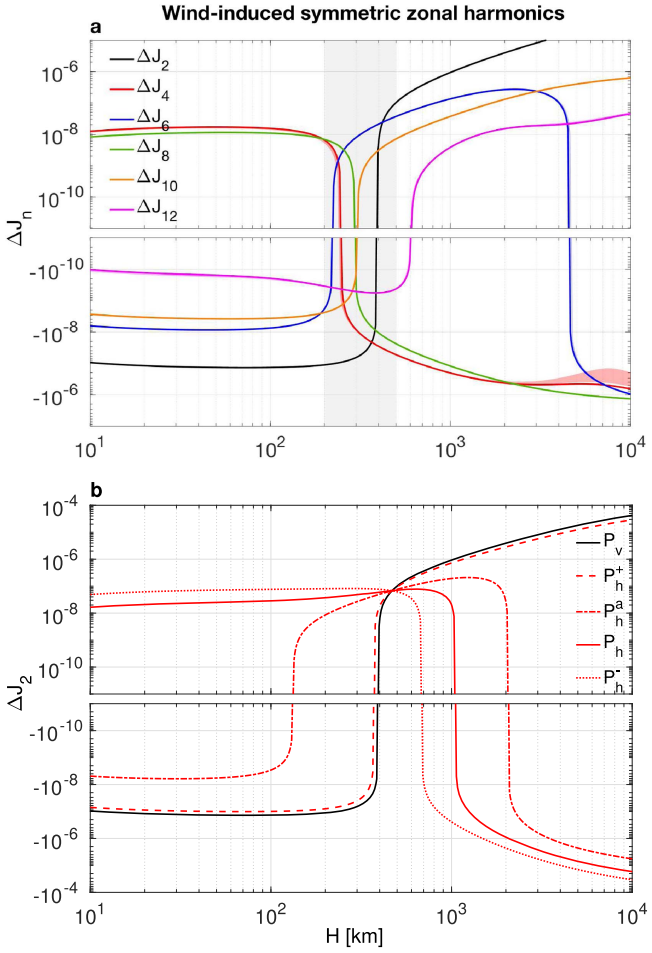

Figure 4. (a) Symmetric zonal harmonics ΔJ_2, ΔJ_4,…, ΔJ_{12} as a function of the decay depth H. Aside from ΔJ_2, all lines are accompanied by a shaded area corresponding to the uncertainty in the cloud-level wind. The shaded area of ΔJ_4 is evident for high values of H, while all other shadings are indistinguishable. The gray shaded area denotes the region where the harmonics change sign. (b) ΔJ_2 as function of H, for different rotation periods.

We also give a prediction for the flow-induced even harmonics ΔJ_2, ΔJ_4,…, ΔJ_{12} as function of the decay depth. We find that the rotation period substantially affects J_2, but has very little effect on the higher-degree even harmonics. This prediction is not expected to be validated directly from the *Cassini* measurements (aside maybe from ΔJ_{10} and ΔJ_{12}), but rather to provide uncertainties to better constrain the internal models used to calculate the total even harmonics (e.g., Kaspi et al. 2017; for the case of Jupiter). Note that modifying the rotation period will also have a significant effect on the static-induced even harmonics, via the modification of the density structure and planet shape (Helled & Guillot 2013). This effect, however, is beyond the scope of this study.

The analysis presented in this study can be used to get a first-order estimate of the flow structure when the *Cassini* Grand Finale measurements arrive by analyzing mainly the odd gravity harmonics. In addition, predicted flow-induced even harmonics can serve as uncertainties for better constraining models of Saturn's static interior density structure. Note that a detailed analysis might also be needed to include additional complexities such as variations of the decay depth with latitude, other vertical decay functions, and possibly even

decoupled interior deep flows (Galanti & Kaspi 2016, 2017; Galanti et al. 2017b).

This research has been supported by the Israeli Ministry of Science, the Minerva foundation with funding from the Federal German Ministry of Education and Research, and the Helen Kimmel Center for Planetary Science at the Weizmann Institute of Science.

References

Anderson, J. D., & Schubert, G. 2007, Sci, 317, 1384
Cao, H., & Stevenson, D. J. 2017, JGRE, 122, 686
Fortney, J. J., & Nettelmann, N. 2010, SSRv, 152, 423
Galanti, E., Durante, D., Finochiaro, S., Iess, L., & Kaspi, Y. 2017a, AJ, 154, 2
Galanti, E., & Kaspi, Y. 2016, ApJ, 820, 91
Galanti, E., & Kaspi, Y. 2017, Icar, 286, 46
Galanti, E., Kaspi, Y., & Tziperman, E. 2017b, JFM, 810, 175
Garcia-Melendo, E., Perez-Hoyos, S., Sanchez-Lavega, A., & Hueso, R. 2011, Icar, 215, 62
Guillot, T. 2005, AREPS, 33, 493
Gurnett, D. A., Kurth, W. S., Hospodarsky, G. B., et al. 2005, Sci, 307, 1255
Helled, R., Galanti, E., & Kaspi, Y. 2015, Natur, 520, 202
Helled, R., & Guillot, T. 2013, ApJ, 767, 113
Hubbard, W. 1982, Icar, 52, 509
Hubbard, W. B. 1999, Icar, 137, 357
Jacobson, R. A., Antreasian, P. G., Bordi, J. J., et al. 2006, ApJ, 132, 2520
Kaspi, Y. 2013, GeoRL, 40, 676
Kaspi, Y., Davighi, J. E., Galanti, E., & Hubbard, W. B. 2016, Icar, 276, 170
Kaspi, Y., Flierl, G. R., & Showman, A. P. 2009, Icar, 202, 525
Kaspi, Y., Guillot, T., Galanti, E., et al. 2017, GeoRL, in press
Kaspi, Y., Hubbard, W. B., Showman, A. P., & Flierl, G. R. 2010, GeoRL, 37, L01204
Kong, D., Zhang, K., & Schubert, G. 2016, Icar, 277, 416
Liu, J., Schneider, T., & Fletcher, L. N. 2014, Icar, 239, 260
Pedlosky, J. 1987, Geophysical Fluid Dynamics (Berlin: Spinger)
Read, P. L., Dowling, T. E., & Schubert, G. 2009, Natur, 460, 608
Sanchez-Lavega, A., Rojas, J. F., & Sada, P. V. 2000, Icar, 147, 405
Schneider, T., & Liu, J. 2009, JAtS, 66, 579
Smith, B. A., Soderblom, L., Batson, R., et al. 1982, Sci, 215, 505
Wahl, S. M., Hubbard, W. B., Militzer, B., et al. 2017, GeoRL, 44, 4649
Zhang, K., Kong, D., & Schubert, G. 2015, ApJ, 806, 270